

Ionochromism, Solvatochromism and Effect of Dissolved Gases on the Spectral Properties of Bromothymol Blue

Duccio Tatini,¹ Erasmo Anselmi,¹ Giacomo Cabrucci,¹ Mert Acar,¹
Barry W. Ninham,² Pierandrea Lo Nostro^{1,*}

- 1: Department of Chemistry and CSGI, University of Florence, 50019 Sesto Fiorentino (Firenze), Italy
- 2: Department of Applied Mathematics, Research School of Physical Sciences and Engineering, Australian National University, ACT 0200 and School of Science, UNSW Canberra, Northcott Drive, Canberra ACT 2610, Australia

*: corresponding author. Email: pierandrea.lonostro@unifi.it

Abstract.

The color of the pH indicator Bromothymol blue (BTB) changes from yellow to blue with increasing pH. The effect of some electrolytes (LiCl, NaCl, KCl, CsCl, KSCN and KClO₃) and of D₂O on the spectral properties of dilute solutions of BTB is explored. The results are interpreted in terms of dimerization of the dye molecules and of the different hydration that D₂O induces.

The effects of dissolved gases on the spectral properties of BTB is studied. Complete removal of dissolved gas is achieved. Surprising effects on the UV-vis spectra emerged. After degassing solutions, gases were re-admitted via bubbling. The gases He, Ar, N₂, CO₂ and CH₄ were studied.

The effects can be explained by presence or absence of nano- and microbubbles of gas in the solution. These allow formation of dimers and multiple association via adsorption and so affect the spectral properties of the dye molecules.

Keywords.

bromothymol blue, self-association of dyes, specific ion effect, dissolved gases, heavy water

Introduction.

General Remarks. Bromothymol blue (BTB) is a derivative of triphenylmethane, it belongs to the group of sulfonphthaleins and is used in several applications [1-6].

BTB is a halochromic dye, blue in alkaline solutions and yellow in an acidic environment (see Figure 1).

BTB is a commonly used acid-base indicator, with $pK_a \approx 7.5$. However the relationship between the chemical structure and the color is still not settled [7].

At low pH (below 7), BTB is stable in solution in yellow form - a monovalent anion with a quinoid structure. It exhibits an absorption maximum at 433.0 nm. The blue form - a divalent anion with a more extended π electron conjugation - shows a peak at 615.5 nm. It is normally stable at high pH (above 7). The blue form is a resonant quinoid-phenolate hybrid as shown in Figure 1.

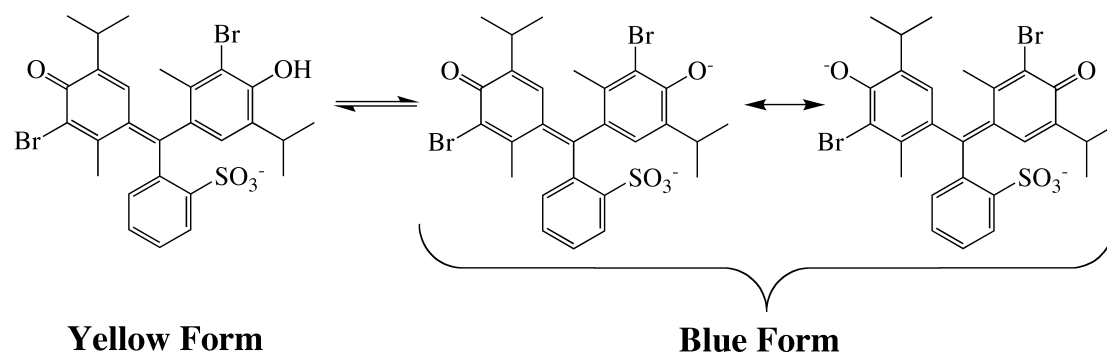


Figure 1. Protolysis equilibrium between acidic (yellow) and basic (blue) forms of bromothymol blue (BTB) and resonant forms at high pH. $pK_a \approx 7.5$.

Figure 2 shows the UV-vis absorbance spectrum of BTB at different pH between 4.5 and 11 [7]. The peaks centered at λ_1 and λ_2 (433 and 616 nm, respectively) correspond to the absorption of the yellow and blue forms, respectively. When the pH increases λ_1 undergoes a strong hypochromic effect and a blue shift, while λ_2 becomes the dominant peak but maintains the same position on the λ axis. Two isosbestic points appear at 324.5 nm and 498.5 nm, These imply that the spectral variations depend on

the equilibrium of only two chemical constituents [7]. However the presence of other very dilute BTB species (10^5 times less concentrated) can be expected on the basis of the deconvolution of the spectrum [7].

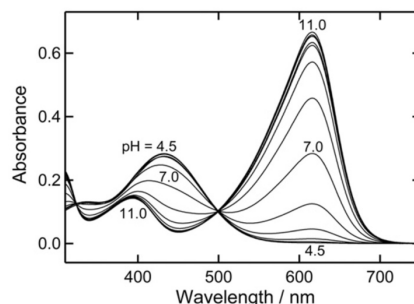


Figure 2. UV-vis absorption spectrum of BTB at different pH. Reprinted from Ref. 7, Copyright 2017, with permission from Elsevier.

Ionochromism. The color of dyes can be significantly altered by changes in physical or chemical conditions, termed chromotropism. The phenomenon can be further classified as thermochromism, solvatochromism, piezochromism, photochromism, ionochromism, halochromism and electrochromism. The different names denote that the physico-chemical changes are triggered by temperature, nature of the solvent, pressure, irradiation, ions, pH or a redox reaction, respectively [8]. In particular, a change in the polarity of the solvent or in the solvation of the chromophore may result in the stabilization of the fundamental state, leading to a hypsochromic (or blue) shift [9,10]. On the other hand, a more stable excited state brings about a bathochromic (or red) shift [9].

The applications of these phenomena in different fields have been widely investigated and exploited [11].

Ionochromism refers to the change of spectral properties of a chromophore upon addition of electrolytes [11]. Both cations and anions contribute to the phenomenon.

The anions are more effective as they have larger polarizabilities than cations.

So they are more efficient in perturbing the electron cloud of the chromophore [12].

Specific ion (Hofmeister) phenomena are ubiquitous. They exist in bulk solutions and at interfaces, in water and in non-aqueous solutions, and consist in the different effect imparted by a specific salt on a particular system depending on the nature of the salt [13]. Usually, but not always, they occur at salt concentrations larger than 10-100 mM, when purely electrostatic models (*e.g.* the Debye-Hückel theory) are dominated by specific stronger ion-ion and ion-solvent interactions. These are due to dispersion and hydration determined by these and other competing short ranged forces [14,15]. While ionochromism for BTB solutions has been documented [16,17], a systematic study on specific ion (Hofmeister) and solvent effects is absent.

Aggregation of dyes. Self-association is a typical feature of dyes in solution [17]. A variety of intermolecular interactions bring about the formation of dimers or larger aggregates [18-22]. Schill reported that BTB ($60 \mu\text{M}$ in water) undergoes self-association and forms dimers and tetramers depending on the concentration of the counterion [23]. BTB like solochrome black and orange II with which it shares some structural features, can also form micelles above the CMC (2.7 mM). Interestingly, when the concentration of sodium ions is as low as 10 mM signs of association can be traced in BTB. For $[\text{Na}^+]$ between 15 and 70 mM colloidal aggregates are formed as indicated by the onset of turbidity [23]. Dutta *et al.* investigated the effect of sodium dodecylsulfate (SDS) on BTB, and found that an increment in the concentration of surfactant is equivalent to a pH lowering. This suggests a strong adsorption of the yellow form of the dye at the interface of the surfactant micelles, which causes the disappearance of the BTB blue form [24].

Aggregates can be of two kinds, termed H and J forms depending on the orientation of the monomeric units. H structures are aligned in parallel face-to-face, and J-structures have head-to-tail arrangements in line, respectively [17].

The formation of aggregates leads to spectral shifts that can be used to quantify their equilibrium constant. In several cases the spectral responses of the monomers and of the aggregates overlap considerably, making the calculation of the equilibrium constant more difficult [25-28].

Salts promote the self-association of dye monomers [29]. This phenomenon has been ascribed to the depression of Coulomb repulsion due to charge screening effects, to hydrophobic interactions [29] and to the different hydration that depends on the specific counterion [17]. The effect of monovalent cations, including some tetraalkylammonium ions, has been classified depending on their radius, enthalpy and entropy of dimerization [29].

Interestingly the thermodynamic parameters of dimerization were found to parallel those of the viscosity Jones-Dole viscosity B coefficient and with the activation energy for viscous flow of the ions [29]. These findings confirm the expected role of specific hydration forces and local water structure around the ions in determining the effect of ion specific dimerization and spectral features of the dye. Some studies on the effect of the solvent and of some additives on the dimerization of thionine seem to confirm that the additive-dye or the solvent-dye interactions (including hydration and dispersion forces) affect the formation of the dimers [29].

Dissolved gases. The removal of dissolved gases from liquids brings about significant changes in their bulk and interfacial properties. It has been shown that when atmospheric gases are stripped away, water becomes a better cleaning agent against hydrophobic dirt [30]. Surprisingly, water/alkane, water/fluorocarbon and even

alkanes/fluorocarbon emulsions are more stable when the liquids are completely degassed [31]. There has been no study until now of the effect of dissolved gases on the spectral properties of a chromophore.

Given this background above we have investigated three different ionochromic and solvatochromic phenomena on change the spectral properties of aqueous BTB solutions. These are;

- (i) the replacement of water with heavy water,
- (ii) the addition of some salts, and
- (iii) the effect of dissolved gases.

We show that these changes induce significant effects on the UV-vis absorbance spectrum of BTB. We explore how they can be related to the formation of self-associated species of the dye in solution.

Materials and Methods.

Chemicals. Deionized purified Milli-Q water from Millipore with a resistivity of 18.2 M Ω and a conductivity of 0.055 S/cm was used in all experiments. Anhydrous LiCl, NaCl, KCl, CsCl, KSCN, KClO₃ (purity \geq 99%) and deuterium oxide (purity 99.9%) were purchased from Merck-Sigma-Aldrich (Milan, Italy), bromothymol blue (BTB, purity 97%), 0.4%) was purchased from Carlo Erba Reagents (Milan, Italy).

Removal of the dissolved gases. The removal of dissolved gases from an aqueous medium was carried out with the Freeze-Pump-Thaw procedure (FPT). The entire multistep process was repeated at least twice. In the first step the liquid is poured in a Pyrex tube and frozen in liquid nitrogen in a Dewar for at least 15 mins, then in the second step the vacuum valve is open to pump out the air and then the dissolved gases through the ice cracks, with an optimal pressure range between 10⁻⁴ and 10⁻⁷ atm. This

step lasts 90 mins after which the vacuum valve is closed again. The last step is meant to return the sample to ambient temperature and pressure and is obtained by gently warming the frozen liquid with a blow dryer. Finally the vacuum valve is very slightly loosened in order to remove the last portion of gas in equilibrium with the liquid.

The vacuum apparatus (Figure 3) comprises a rotary pump with two-stage vanes, model RV 25D (Arcatec srl, Cologno Monzese, Italy), with a circulating lubricant oil. A high-vacuum tube (Disa sas, Milan, Italy) is connected to the pump through a Rotulex 19/9 junction. In between, a liquid nitrogen trap is located to block water vapors and improve the efficiency of the pump.

The pump nominal rate is 5.4 m³/h with a final pressure of 2 mbar and a motor power of 0.12 kW.



Figure 3. High vacuum apparatus used for the removal of the dissolved gases from a liquid.

pH measurement. The pH meter (Waterproof SMTE00K4) was calibrated with standard buffers at pH 4 and 7.

UV-vis spectrophotometry. The absorbance spectra of the aqueous solutions of BTB in the presence of salts, heavy water, and after removing the dissolved gases, were acquired using a UV-vis Cary 3500 (Agilent Technologies Italia SpA, Milan, Italy).

The temperature was kept constant at 25.0 ± 0.1 °C.

Figure 4 shows three cuvettes that contain from left to right the BTB-free KCl aqueous solution, the 0.50 M KCl solution with BTB before degassing, and the same sample after the removal of the dissolved gases, respectively.

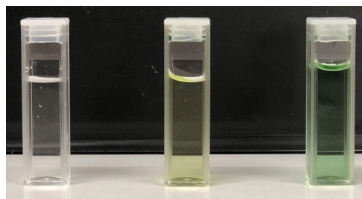


Figure 4. From left to right: the BTB-free KCl aqueous solution, the KCl solution with BTB before degassing, and the KCl solution with BTB after the removal of the dissolved gases. $[\text{KCl}] = 0.50 \text{ M}$.

Results and Discussion.

Water/heavy water. BTB was dissolved in different mixtures of $\text{H}_2\text{O}/\text{D}_2\text{O}$ (0, 25%, 50%, 75% and 100% v/v in D_2O) keeping the same concentration of the dye ($6.4 \mu\text{M}$) and the UV-vis absorption spectra were recorded in the same experimental conditions. A picture of the samples is shown in Figure S1 in the Supplementary Material, and the spectra are shown in Figure 5. Peak 1 ($\lambda_1 \approx 420 \text{ nm}$) undergoes a hypsochromic (or blue) shift and a moderate hypochromic effect as the content of D_2O in the solvent increases. These findings were obtained also in the case of squaraine dyes dissolved in D_2O [32]. In contrast, for peak 2 ($\lambda_2 \approx 620 \text{ nm}$) the position of the peak remains constant and a remarkable hyperchromic effect takes place. See Table 1 for the changes in wavelength and absorbance of each sample.

Table 1. Spectral parameters for BTB in H₂O/D₂O mixtures for the investigated volume ratios.

H ₂ O:D ₂ O v/v	λ_1 (nm)	A_1	λ_2 (nm)	A_2
1.00	488.3	0.0982	615.8	0.0447
0.75	425.4	0.0820	615.8	0.0555
0.50	424.6	0.0847	615.1	0.0575
0.25	421.7	0.0807	615.8	0.0684
0.00	417.1	0.0795	615.8	0.0869

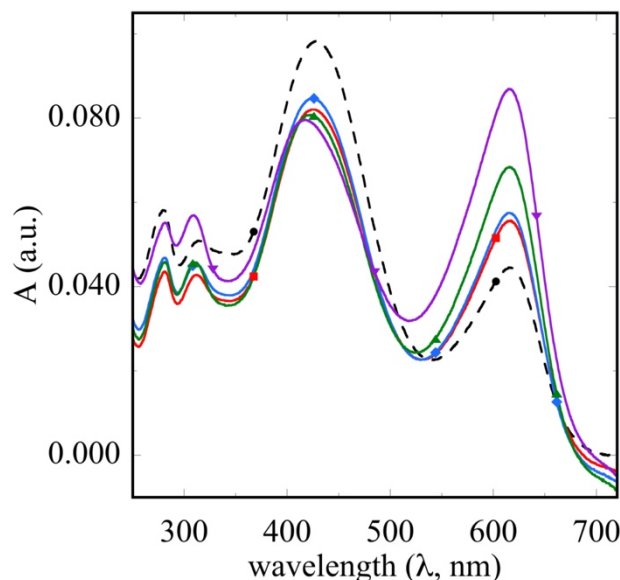


Figure 5. UV-vis absorption spectra of BTB dissolved in water (dotted black line, ●), in D₂O (▼) and in D₂O/H₂O mixtures with a volume ratio of 0.25 (■), 0.50 (◆), and 0.75 (▲).

The results indicate that as the heavy water content increases the alkaline (blue) form of BTB is more stable. The color of the solution turns progressively greener and eventually to light blue. Figure S2 in the Supplementary Material shows that the addition of D₂O slightly decreases the wavelength of peak 1 progressively (red triangles). At the same time it leaves the position of peak 2 at higher wavelength unperturbed (red circles). Instead the effect of heavy water on the absorbance of peak 2 is stronger (blue circles) with a significant hyperchromic effect as the content of D₂O increases.

It has been reported that the blue shift of peak 1 can be related to the formation of H-dimers [17]. This result implies that the addition of even small amounts of heavy

water significantly modifies the hydration of the BTB monomers and promotes their self-association. In fact the observed spectral changes can be explained assuming (i) a conformational transition that involves extended conjugation (particularly in the case of the resonant structures in the blue form), (ii) the self-association of the chromophore monomers in aggregates, and (iii) an intramolecular folding [33].

These conclusions are in line with previous findings showing that the stacking of dye molecules in dimers and higher aggregates is promoted by the replacement of water with D₂O [34], due to the stronger hydrogen bonding and polarity of D₂O respect to H₂O [35,36].

Effect of salts. The UV-vis spectra of BTB were recorded in the presence of a number of strong electrolytes under the same experimental conditions. We investigated the effect of some alkali metal chlorides (LiCl, NaCl, KCl and CsCl) and of KSCN and KClO₃ at two different concentrations, 0.01 and 0.50 M. The first four salts were selected to study the effect of the cation in 1:1 electrolytes keeping the same anion. These ion pairs all inhibit bubble bubble fusion above physiological salt concentrations, 0.17 M [31,37]. The last two potassium salts were chosen because they belong the class of ion pairs that have no effect on bubble fusion [37]. Figures 6 ([salt] = 0.01 M) and 7 ([salt] = 0.50 M) show the samples investigated, while figures 8 ([salt] = 0.01 M) and 9 ([salt] = 0.50 M) show the UV-vis absorption spectra of the samples. The dye concentration is kept at $6.4 \cdot 10^{-6}$ M.

Table 2 lists the spectral parameters (absorbance A and wavelength λ) for the two peaks centered at about 430 and 616 nm, for all samples at concentrations 0.01 and 0.50 M.

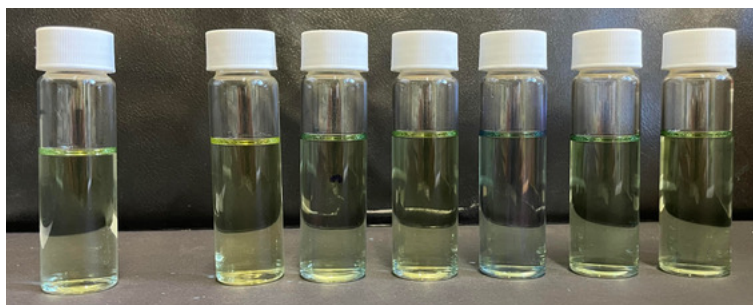


Figure 6. From left to right: BTB in pure water and in 0.01 M aqueous LiCl, NaCl, KCl, CsCl, KSCN and KClO₃. [BTB] = 6.4·10⁻⁶ M.

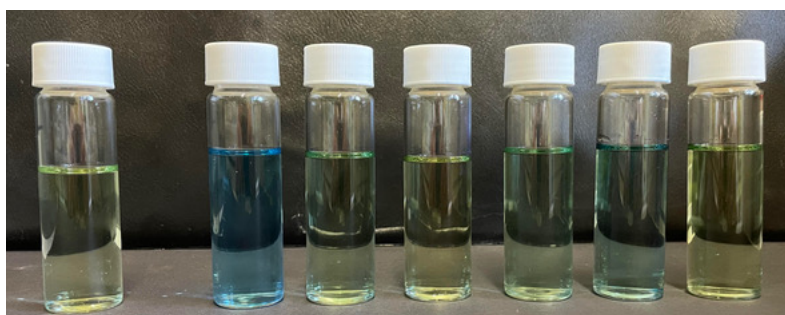


Figure 7. From left to right: BTB in pure water and in 0.50 M aqueous LiCl, NaCl, KCl, CsCl, KSCN and KClO₃. [BTB] = 6.4·10⁻⁶ M.

Table 2. Spectral parameters for BTB in water and in aqueous solutions of LiCl, NaCl, KCl, CsCl, KSCN and KClO₃ at 0.01 M and 0.50 M.

	λ_1 (nm)	A_1	λ_2 (nm)	A_2	λ_1 (nm)	A_1	λ_2 (nm)	A_2
	0.01 M				0.50 M			
no salt	428.0	0.0982	616.3	0.0444	428.3	0.0983	616.1	0.0448
LiCl	431.1	0.1180	616.7	0.0110	405.5	0.0687	616.9	0.1400
NaCl	431.4	0.1027	616.3	0.0102	430.5	0.0956	616.1	0.0238
KCl	429.7	0.0992	616.3	0.0227	431.1	0.0949	616.1	0.0182
CsCl	431.1	0.1070	616.7	0.0133	427.8	0.0947	616.7	0.0531
KSCN	429.7	0.0938	616.3	0.0347	423.3	0.0765	616.7	0.0819
KClO ₃	431.9	0.0927	616.3	0.0129	431.7	0.1031	616.7	0.0161

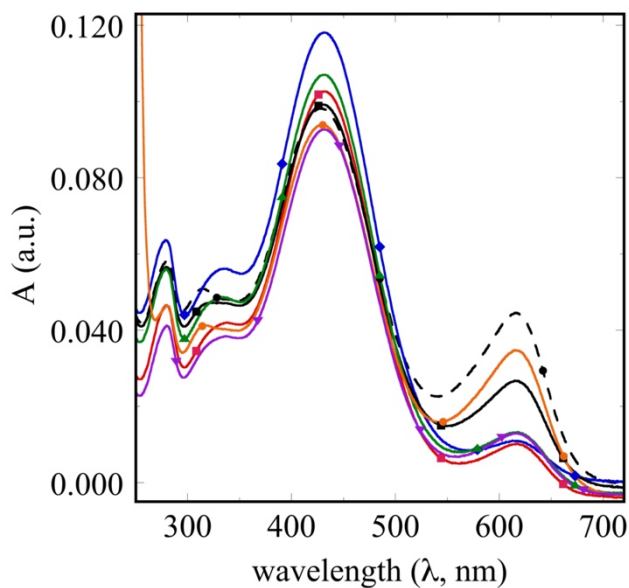


Figure 8. UV-vis spectra of BTB in pure water (dotted black line, ●), LiCl (◆), NaCl (■), KCl (■), CsCl (▲), KSCN (●) and KClO₃ (▼). [BTB] = $6.4 \cdot 10^{-6}$ M, [salt] = 0.01 M.

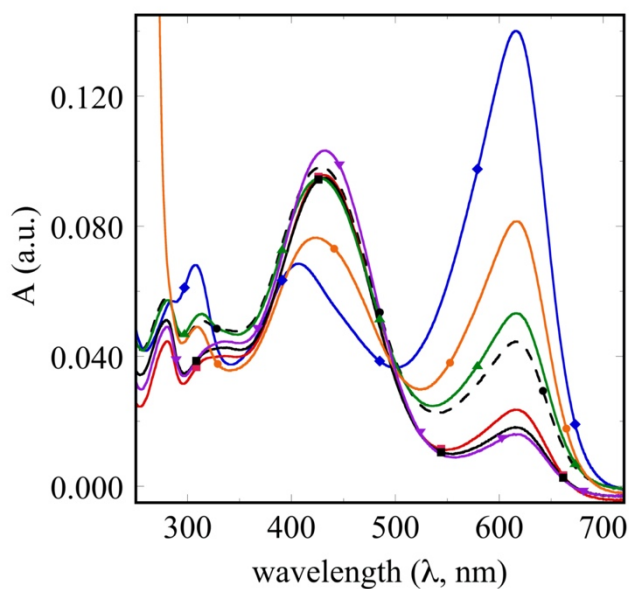


Figure 9. UV-vis spectra of BTB in pure water (dotted black line, ●), LiCl (◆), NaCl (■), KCl (■), CsCl (▲), KSCN (●) and KClO₃ (▼). [BTB] = $6.4 \cdot 10^{-6}$ M, [salt] = 0.50 M.

At 0.01 M the effect of the salts is small, in fact no wavelength shift is recorded for the two peaks. Concerning the absorbance, all salts produce a strong hypochromic effect respect to pure water (dotted line in Figures 8 and 9). Instead, at 430 nm we observed a regular increase in the absorbance as:



A much stronger effect on the spectra is seen when the concentration of the salts is raised to 0.50 M. LiCl has a tremendous effect, with a strong hypsochromic and hypochromic shift for peak 1, that can probably be ascribed to the formation of H-aggregates [32,38]. There is an enormous increment in the absorbance at 616 nm although no pH change is recorded. These effects can be summarized as follows:

wavelength for peak 1: $\text{KClO}_3 > \text{NaCl}, \text{KCl} > \text{water} > \text{CsCl} > \text{KSCN} > \text{LiCl}$

absorbance for peak 1: $\text{KClO}_3 > \text{water} > \text{NaCl}, \text{KCl}, \text{CsCl} > \text{KSCN} > \text{LiCl}$

wavelength for peak 2: no effect

absorbance for peak 2: $\text{LiCl} > \text{KSCN} > \text{CsCl} > \text{water} > \text{NaCl} > \text{KCl}, \text{KClO}_3$.

Lithium and cesium chlorides are special cases, with the most significant changes in the spectra. A previous study on the alkali metal- π interactions through IR and computations shows that Li^+ establishes strong interactions with phenols and significantly perturbs the stability of the dimers [39]. Instead, Cs^+ is not able to destroy the phenol intermolecular hydrogen bonds and rather stabilizes other kinds of associates [40]. We argue that also in our system these two cations interfere with the formation of BTB dimers via the phenol units. In particular the specific interactions between Li^+ or Cs^+ with the negative charges of BTB can reduce the repulsion between dye molecules and favor their association [41].

If the effect of Li^+ and Cs^+ on the spectral properties of BTB can be explained by invoking cation-dye interactions, and in particular the interaction between Li^+ and negatively charged residues (phenolate and sulfonate), and cation- π interactions between Cs^+ and the aromatic backbone. Similarly the effect of thiocyanate can be interpreted in terms of anion- π interactions [12]. As reported by Wang and Wang, 1:1 complexes are formed by an electron-deficient aromatic molecules such as tetraoxacalix[2]arene[2]-triazine with some polyatomic anions of different geometries

and shapes in the gaseous phase, in solution, and in the solid state. Among these anions, thiocyanate interacts with the aromatic molecule through cooperative anion- π and lone-pair electron- π interactions [42]. We argue that the high polarizability of SCN^- (6.47 \AA^3) [43], that reflects the diffuse electron cloud around the anion, and the aromatic molecular orbitals of BTB promote the formation of relatively strong interactions between the anion and the dye molecule, both in the monomeric form and in the aggregates. Thiocyanate can even act as an anionic bridge between two facing BTB molecules [44]. These interactions might result in the changes of the spectral features that we detected and show in Figure 9.

We observe that the absorbance for peak 1 and peak 2 (A_1 and A_2 , respectively) increases with the Jones-Dole viscosity B coefficient (B_{JD}) of the cation and of the anion [45]. The values of B_{JD} for the cations and anions used in this study were taken from Ref. 46. The concentration dependence of viscosity for an aqueous solution is given by equation 1:

$$\eta = \eta_0(1 + a\sqrt{c} + B_{JD}c) \quad (1)$$

where η , η_0 , and c are the viscosity of the salt solution, the viscosity of pure water at the same temperature. The coefficient a accounts for electrostatic interactions. B_{JD} reflects the effect of an ion on the viscosity of its solutions: cosmotropes possess positive values of B_{JD} (the solution is more viscous than water at the same temperature), whereas chaotropes show negative values for B_{JD} and make the solution more fluid.

In brief, the correlation of A_1 and A_2 for the BTB solutions with 0.50 M salts suggest that the effect of the electrolytes is related to the hydration properties of their constituting ions [41]. In turn, a change in the hydration features of BTB upon

addition of a salt can justify the recorded spectral variations especially in terms of changes in the π conjugation and in terms of the dye self-association [32].

Dissolved gases.

Removal of dissolved gases. The removal of dissolved gases has intriguing effects in many systems such as those reported in the literature [31,47,48]. Here we show that degassing brings about some interesting changes in the spectral properties. This is the first time that such effects have been studied.

We will first report the effects of stripping out the gas. We used the procedure described in the Materials and Methods section. Later we follow this up the effect by reversing the procedure, admitting different gases into the solution.

Figure 10 shows three samples: from left to right, a 0.5 M aqueous solution of KCl in the presence of BTB as it appears and after 2 and 4 cycles of FPT.

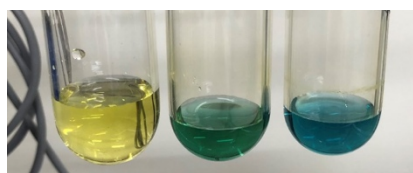


Figure 10. From left to right: color of a 0.50 M aqueous solution of KCl in the presence of BTB as it is and after 2 and 4 cycles of FPT.

Apparently with two cycles of freeze-pump-thaw the removal of dissolved gases leads to the typical green color of BTB for $\text{pH} \approx 7$. But when the sample is treated with two more FPT cycles the color turns blue. Figure E shows the UV-vis spectra of a untreated (blue curve) and of a degassed (red curve) sample containing 0.50 M KCl in water and BTB. After the removal of degassed gases a blue shift from 427 to 424.5 nm occurs while the peak at 617.5 nm increases significantly, as shown in Figure 11. Above 0.50 M we expect nanobubbles to form, at which the dye will adsorb and “see” a different environment to that in the bulk and at 0.01 M molar (below the critical

concentration for nanobubble formation). The nanobubble formation depends on amount of dissolved gas left [31].

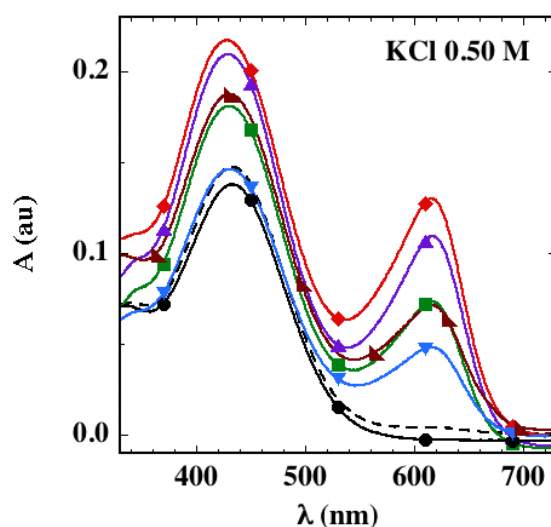


Figure 11. Absorption spectra of BTB in 0.50 M KCl on: untreated sample (dotted line), degassed (♦), and after re-admittance of He (■), N₂ (▲), CO₂ (●), Ar (▼) and CH₄ (▴).

After re-admitting air through the valve the color slowly reverts from green to yellow overnight.

The 0.01 M solution of KCl shows analogies but also disparities with respect to the more concentrated sample KCl. The absorption spectra (see Figure 12) indicates a blue shift from 430 to 426.5 nm upon degassing, while the peak at 618 nm appears only after the removal of the dissolved gases.

The only significant difference between the two KCl solutions is the rate of CO₂ adsorption when air is re-admitted into the sample: the process is much faster in the 0.5 M KCl sample as it was proved by running the kinetic profile of λ_1 as a function of time on the sample left in contact with air.

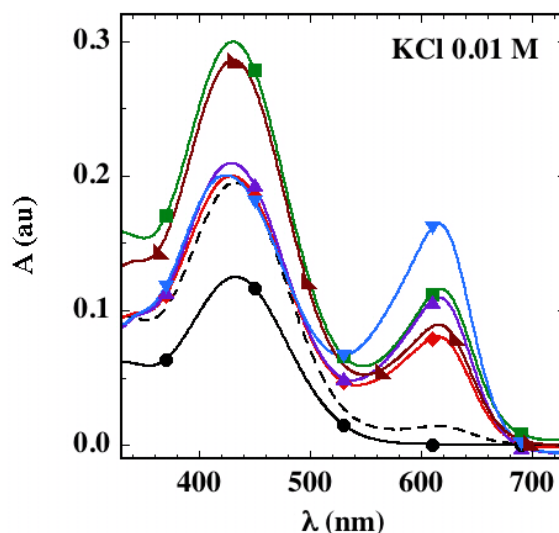


Figure 12. Absorption spectra of BTB in 0.01 M KCl on: untreated sample (dotted line), degassed (◆), and after re-admittance of He (■), N₂ (▲), CO₂ (●), Ar (▼) and CH₄ (▴).

Re-admittance of gases.

Table 3 lists the values of λ_1 and λ_2 extracted from the absorption spectra performed on the different systems: untreated and degassed KCl solutions (0.01 M and 0.50 M), and after re-admittance of nitrogen, carbon dioxide, argon, methane and helium at 1.3 bar at 20° C for 30 mins. The removal of the dissolved gases brings about the appearance of the new peak at about 616 nm. The spectra are reported in Figures 11 and 12.

The differences between the untreated and degassed samples are larger, and the re-admission of single gases has a greater impact in the case of the more concentrated KCl solution. Peak 1 remains almost unperturbed in 0.01 M KCl no matter what gas is bubbled through the solution, while in 0.50 M KCl the effect correlates with the saturation of the gas in water at 298.15 K and 1 atm (x_{sat}) and with the polarizability of the gas, α (see Table 3). The observation is relevant because van der Waals interactions directly depend on the polarizabilities and on the dipole moments of the

interacting particles [13]. Larger polarizabilities can participate in the strengthening of interactions that involve aromatic backbones, ions and neutral molecules.

Peak 2 disappears in the presence of CO₂, while it remains at the same λ_2 value with the other gases.

It is interesting to observe that helium, one the least soluble gases in water, leads to values of λ_1 and λ_2 very similar to the degassed solutions.

Table 3. Equilibrium solubility (as mole fraction x_{sat}) of the investigated gases in water at 298.15 K and 1 atm and their experimental polarizabilities (in Å³), values of λ_1 and λ_2 (in nm) extracted from the absorption spectra.

	x_{sat}^a	α	λ_1	λ_2	λ_1	λ_2
			0.01 M KCl		0.50 M KCl	
untreated (air)			432.0	-	434.0	-
degassed			430.0	616.0	428.5	615.5
He	$6.997 \cdot 10^{-6}$	0.21 ^b	430.5	617.5	428.5	616.5
Ar	$2.796 \cdot 10^{-5}$	1.63 ^b	430.5	616.0	429.0	617.5
N ₂	$1.183 \cdot 10^{-5}$	1.73 ^b	429.5	617.0	429.0	615.5
CH ₄	$2.552 \cdot 10^{-5}$	2.45 ^c	430.5	616.0	430.0	616.0
CO ₂	$6.15 \cdot 10^{-4}$	2.63 ^d	433.0	-	433.0	-

a: from Ref. 49; b: from Ref. 47; c: from Ref. 50; d: from Ref. 51.

The detected shifts in the wavelength of the UV-vis peaks can be interpreted in at least in two different ways. We observed that the value of λ_1 , that corresponds to the yellow (acidic) form of BTB undergoes a blue shift when the solution is degassed and even more so when the single gases are re-admitted. The exception is CO₂. On the other hand the peak of the blue (basic) form of BTB does not significantly change with the individual gases; it just disappears in the presence of CO₂ as in the untreated, air saturated solutions. The blue shift of λ_1 might be explained by invoking a change in the spectral properties of BTB due to partial association of the monomers into dimers and tetramers as a result of strong π -stacking interactions between two or more adjacent molecules of the dye, due to the extended π conjugation in the BTB molecule [23,52].

In order to explain these results we recall that, as we anticipated in the Introduction, BTB self-associates in the presence of SDS [24]. Moreover we recall that the removal of dissolved gases from an oil-in-water emulsion induces a similar effect produced by the addition of a surfactant [17,53]. By analogy, we propose that the removal of the dissolved gases leads to the self-association of BTB molecules as in the case of BTB/SDS mixtures. Basically in our views the air nano- and microbubbles dissolved in the solution stabilize the dye molecules in the monomeric forms, through the adsorption of the dye's aromatic backbone at the hydrophobic interface of the bubbles. This is particularly evident when the background salt concentration is 0.50 M. When the bubbles are stripped off, the dye monomers ought to self-associate - at least in part - due to hydrophobic effects.

Conclusions.

We investigated the effects of D₂O, of various salts and of different gases on the UV-vis spectral properties of a pH indicator, bromothymol blue (BTB), in water at a very low concentration, $6.4 \cdot 10^{-6}$ M. The results indicate that the dye solution turns from yellow to blue in the following cases:

- i. When D₂O replaces H₂O.
- ii. When Li⁺, Cs⁺ and SCN⁻ ions are added to the solution
- iii. When the solution is degassed.

The effect induced by heavy water is related to the higher energy of its hydrogen bonds, and therefore the spectral changes ultimately occur because of the hydration of the ionic residues (phenolate and sulfonate) in the dye molecules. Similar dramatic effects have been explored with the fuel cell polymer nafion [53-56].

Hydration is also involved in the lithium-BTB interaction, while the effect of cesium and thiocyanate are due to a strong cation- π and an anion- π interaction, respectively. All these interactions result in a significant perturbation of the energy levels of the monomer and dimers, and therefore induce the spectral shifts that can be seen in the visible spectrum.

Dissolved gases are reminiscent of the addition of a surfactant, associating to form nanobubbles and microbubbles formed by aggregation of nanobubbles. They form a platform on which the dye can adsorb and associate. On removal of gas, through the same hydrophobic effect, self-association of the dye molecules occurs differently in order to minimize the exposure to water.

While the effect of heavy water and of some electrolytes on the UV-vis absorption of dyes has already been reported in the literature, this work highlights for the first time the significance of dissolved gases in solutions generally. The effects show up strongly in the spectral properties of bromothymol blue. Many more experiments are needed to further clarify these observations, for example the relevance of dissolved gases on hydrophobic chromophores in organic solvents.

Finally the different effect of alkali metal cations, especially Li^+ compared to Na^+ and K^+ is part of a well-known field, still to be explored, where specific interactions (ion- π , hydration and hydrophobic forces) conspire in the modulation of several biological mechanism, such as the Na^+/K^+ gradient across membranes, the effect of lithium in neurological diseases [57], and more.

References.

1. T. De Meyer, K. Hemelsoet, L. Van der Schueren, E. Pauwels, K. De Clerck, V. Van Speybroeck, Investigating the halochromic properties of azo dyes in an aqueous environment by using a combined experimental and theoretical approach, *Chem. Eur. J.* 18 (2012) 8120–8129.
2. T. De Meyer, K. Hemelsoet, V. Van Speybroeck, K. De Clerck, Substituent effects on absorption spectra of pH indicators: an experimental and computational study of sulfonphthaleine dyes, *Dyes Pigments* 102 (2014) 241–250.
3. G.J. Mohr, O.S. Wolfbeis, Optical sensors for a wide pH range based on azo dyes immobilized on a novel support, *Anal. Chim. Acta* 292 (1994) 41–48.
4. T. Kuwabara, H. Nakajima, M. Nanasawa, A. Ueno, Color change indicators for molecules using methyl red modified cyclodextrins, *Anal. Chem.* 71 (1999) 2844–2849.
5. L. Van der Schueren, K. De Clerck, The use of pH-indicator dyes for pH-sensitive textile materials, *Text. Res. J.* 80 (2010) 590–603.
6. S. Trupp, M. Alberti, T. Carofiglio, E. Lubian, H. Lehmann, R. Heuermann, E. Yacoub-George, K. Bock, G.J. Mohr, Development of pH-sensitive indicator dyes for the preparation of micro-patterned optical sensor layers, *Sensors Actuators B Chem.* 150 (2010) 206–210.
7. T. Shimada, T. Hasegawa, Determination of equilibrium structures of bromothymol blue revealed by using quantum chemistry with an aid of multivariate analysis of electronic absorption spectra, *Spectrochimica Acta Part A: Molecular and Biomolecular Spectroscopy* 185 (2017) 104–110.

8. Y. Fukuda, *Inorganic Chromotropism: basic concepts and applications of colored materials*, Springer, Berlin, 2007.
9. C. Reichardt, Solvatochromic Dyes as Solvent Polarity Indicators, *Chem. Rev.* 94 (1994) 2319-2358.
10. T.J. Zuehlsdorff, C.M. Isborn, Modeling absorption spectra of molecules in solution, *Int. J. Quantum Chem.* 119 (2019) e25719.
11. H. Golchoubian, G. Moayyedi, N. Reisi, Halochromism, ionochromism, solvatochromism and density functional study of a synthesized copper(II) complex containing hemilabile amide derivative ligand. *Spectrochimica Acta Part A: Molecular and Biomolecular Spectroscopy* 138 (2015) 913-924.
12. S. Zanotto, M. Scremin, C. Machado, M.C. Rezedo, Cationic and anionic halochromism, *J. Phys. Org. Chem.* 6 (1993) 637-641.
13. P. Lo Nostro, B.W. Ninham, Hofmeister Phenomena: An Update on Ion Specificity in Biology, *Chem. Rev.* 112 (2012) 2286–2322.
14. B.W. Ninham, V. Yaminsky, Ion Binding and Ion Specificity: The Hofmeister Effect and Onsager and Lifshitz Theories, *Langmuir* 13 (1997) 2097-2108.
15. B.W. Ninham, P. Lo Nostro, *Molecular Forces and Self Assembly*. In *Colloid, Nano Sciences and Biology*; Cambridge University Press, 2010.
16. M. Qiu, S. Long, B. Li, L. Yan, W. Xie, Y. Niu, X. Wang, Q. Qianjin, A. Xia, Toward an Understanding of How the Optical Property of Water-Soluble Cationic Polythiophene Derivative Is Altered by the Addition of Salts: The Hofmeister Effect, *J. Phys. Chem. C* 117 (2013) 21870-21878.
17. B. Heyne, Self-assembly of organic dyes in supramolecular aggregates, *Photochem. Photobiol. Sci.* 15 (2016) 1103-1114.

18. A.K. Chibisov, T.D. Slavnova, H. Gorner, Dimerization kinetics of thiocarbocyanine dyes by photochemically induced concentration jump, *Chem. Phys. Lett.* 386 (2004) 301-306.
19. S. Miljanic, Z. Cimerman, L. Frkanec, M. Zinic, Lipophilic derivative of rhodamine 19: Characterization and spectroscopic properties, *Anal. Chim. Acta* 468 (2002) 13-25.
20. J.C. Micheau, G.V. Zakharova, A.K. Chibisov, Reversible aggregation, precipitation and re-dissolution of rhodamine 6G in aqueous sodium dodecyl sulfate, *Phys. Chem. Chem. Phys.* 6 (2004) 2420-2425.
21. L. Antonov, G. Gergov, V. Petrov, M. Kubista, J. Nygren, UV-Vis spectroscopic and chemometric study on the aggregation of ionic dyes in water, *Talanta* 49 (1999) 99-106.
22. J. Ghasemi, A. Niazi, G. Westman, M. Kubista, Thermodynamic characterization of the dimerization equilibrium of an asymmetric dye by spectral titration and chemometric analysis, *Talanta* 62 (2004) 835-841.
23. G. Schill, Photometric determination of amines and quaternary ammonium compounds with bromothymol blue. Part 2. Association of bromothymol blue in aqueous solutions, *Acta Pharm. Suec.* 1 (1964) 101-122.
24. R.K. Dutta, R. Chowdhury, S.N. Bha, Effect of Association of Sulfonephthalein Dyes with Sodium Dodecyl Sulfate Micelles on Their Acid-Base Equilibria, *J. Chem. Soc Faraday Trans.* 91 (1995) 681-686.
25. I. Baraldi, M. Caselli, F. Momicchioli, G. Pontereini, D. Vanossi, Dimerization of green sensitizing cyanines in solution. A spectroscopic and theoretical study of the bonding nature, *Chem. Phys.* 275 (2002) 149-165.

26. A.G. Gilani, R. Sariri, K. Bahrpaima, Aggregate formation of Rhodamine 6G in anisotropic solvents, *Spectrochim. Acta Part A* 57 (2001) 155-161.
27. M.T.M. Choi, P.P.S. Li, D.K.P. Ng, A direct comparison of the aggregation behavior of phthalocyanines and 2, 3-naphthalocyanines, *Tetrahedron* 56 (2000) 3881-3887.
28. K. Patil, R. Pawar, P. Talap, Self-aggregation of methylene blue in aqueous medium and aqueous solutions of Bu_4NBr and urea, *Phys. Chem. Chem. Phys.* 2 (2000) 4313-4317.
29. K. Murakami, Thermodynamic and kinetic aspects of self-association of dyes in aqueous solution, *Dyes and Pigments* 53 (2002) 31–43.
30. R.M. Pashley, M. Rzechowicz, L.R. Pashley, M.J. Francis, De-Gassed Water Is a Better Cleaning Agent, *J. Phys. Chem. B* 109 (2005) 1231–1238.
31. B.W. Ninham, P. Lo Nostro, Unexpected Properties of Degassed Solutions, *J. Phys. Chem. B* 124 (2020) 7872–7878.
32. S. Das, K.G. Thomas, K.J. Thomas, V. Madhavan, D. Liu, P.V. Kamat, M.V. George, Aggregation Behavior of Water Soluble Bis(benzothiazolylidene)squaraine Derivatives in Aqueous Media, *J. Phys. Chem.* 100 (1996) 17310-17311.
33. M. Qiu, S. Long, B. Li, L. Yan, W. Xie, Y. Niu, X. Wang, Q. Guo, A. Xia, Toward an Understanding of How the Optical Property of Water-Soluble Cationic Polythiophene Derivative Is Altered by the Addition of Salts: The Hofmeister Effect, *J. Phys. Chem.* 117 (2013) 21870-21878.
34. S.L. Fornili, G. Sgroi, L. Palumbo, Effect of Solvent on Stacking Interactions, *J. Chem. Soc. Faraday Trans. 1* 81 (1985) 255-258.

35. C.R. Lopez-Barrón, N.J. Wagner, Solvent isotope effect on the microstructure and rheology of cationic wormlike micelles near the isotropic-nematic transition, *Soft Matter* 7 (2011) 10856-10863.
36. S. Scheiner, M. Cuma, Relative stability of hydrogen and deuterium bonds, *J. Am. Chem. Soc.* 118 (1996) 1511-1521.
37. V.S.J. Craig, B.W. Ninham, R.M. Pashley, The Effect of Electrolytes on Bubble Coalescence in Water, *J. Phys. Chem.* 97 (1993) 10192-10197.
38. D.J. Blears, S.S. Danyluk, The Aggregation of Acridine Orange in Aqueous Solution, *J. Am. Chem. Soc.* 88 (1966) 1084-1085.
39. T.D. Vaden, J.M. Lisy, Competition between cation- π interactions and intermolecular hydrogen bonds in alkali metal ion-phenol clusters. I. Phenol dimer, *J. Chem. Phys.* 123 (2005) 074302.
40. T.D. Vaden, J.M. Lisy, Competition between cation- π interactions and intermolecular hydrogen bonds in alkali metal ion-phenol clusters. II. Phenol trimer, *J. Chem. Phys.* 124 (2006) 214315.
41. E.H. Braswell, Sedimentation and Absorption Spectroscopy Studies of Some Self-Associating Cationic Dyes, *J. Phys. Chem.* 88 (1984) 3653-3658.
42. D.-X. Wang, M.-X. Wang, Anion- π Interactions: Generality, Binding Strength, and Structure, *J. Am. Chem. Soc.* 135 (2013) 892-897.
43. S. Rossi, P. Lo Nostro, M. Lagi, B.W. Ninham, P. Baglioni, Specific Anion Effects on the Optical Rotation of α -Amino Acids, *J. Phys. Chem. B* 111 (2007) 10510-10519.
44. P. Lo Nostro, N. Peruzzi, M. Severi, B.W. Ninham, P. Baglioni, Asymmetric Partitioning of Anions in Lysozyme Dispersions, *J. Am. Chem. Soc.* 132 (2010) 6571-6577.

45. D. Tatini, D. Ciardi, C. Sofroniou, B.W. Ninham, P. Lo Nostro, Physicochemical characterization of green sodium oleate-based formulations. Part 2, Effect of anions. *J. Coll. Interface Sci.* 617 (2022) 399-408.
46. H.D.B. Jenkins, Y. Marcus, Viscosity B-Coefficients of Ions in Solution, *Chem. Rev.* 95 (1995) 2695-2724.
47. M. Lagi, P. Lo Nostro, E. Fratini, B.W. Ninham, P. Baglioni, Insights into Hofmeister Mechanisms: Anion and Degassing Effects on the Cloud Point of Dioctanoylphosphatidylcholine/Water Systems, *J. Phys. Chem. B* 111 (2007) 589-597.
48. A. Becheri, P. Lo Nostro, B.W. Ninham, P. Baglioni, The Curious World of Polypseudorotaxanes: Cyclodextrins As Probes of Water Structure, *J. Phys. Chem. B* 107 (2003) 3979-3987.
49. CRC Handbook of Chemistry and Physics. Chemical Rubber Co.: Ohio, 1970.
50. Experimental Polarizabilities. <https://cccbdb.nist.gov/pollistx.asp>, last accessed on July 22, 2022.
51. M. Lewis, Z. Wu, R. Glaser, Polarizabilities of Carbon Dioxide and Carbodiimide. Assessment of Theoretical Model Dependencies on Dipole Polarizabilities and Dipole Polarizability Anisotropies, *J. Phys. Chem. A* 104 (2000) 11355-11361.
52. B. Liu, H. Ranji-Burachaloo, P. A. Gurr, E. Goudeli, G. G. Qiao, A nontoxic reversible thermochromic binary system via π - π stacking of sulfonephthaleins, *J. Mater. Chem. C* 7 (2019) 9335-9345.
53. G. R. Burnett, R. Atkin, S. Hicks, J. Eastoe, Surfactant-Free “Emulsions” Generated by Freeze-Thaw, *Langmuir* 20 (2004) 5673-5678.

54. N.F. Bunkin, A.V. Shkirin, V.A. Kozlov, B.W. Ninham, E.V. Uspenskaya, S.V. Gudkov, Near-surface structure of Nafion in deuterated water, *J. Chem. Phys.* 149 (2018) 164901.
55. B.W. Ninham, P.N. Bolotskova, S.V. Gudkov, Y. Juraev, M.S. Kiryanova, V.A. Kozlov, R.S. Safronenkov, A.V. Shkirin, E.V. Uspenskaya, N.F. Bunkin, Formation of Water-Free Cavity in the Process of Nafion Swelling in a Cell of Limited Volume; Effect of Polymer Fibers Unwinding, *Polymers* 12 (2020) 2888.
56. R. M. Pashley, Effect of Degassing on the Formation and Stability of Surfactant-Free Emulsions and Fine Teflon, *J. Phys. Chem. B*, 2003, 107, 1714-1720.
57. E. Shorter, The history of lithium therapy, *Bipolar Disorders* 11 (2009) 4-9/